Exact results for persistent currents of two bosons in a ring lattice

Juan Polo,[1,2,*] Piero Naldesi,[2] Anna Minguzzi,[2] and Luigi Amico[3,4,5,6,7]

[1]*Quantum Systems Unit, Okinawa Institute of Science and Technology Graduate University, Onna, Okinawa 904-0495, Japan*

[2]*Université Grenoble Alpes, CNRS, LPMMC, F-38000 Grenoble, France*

[3]*Dipartimento di Fisica e Astronomia, Via S. Sofia 64, I-95127 Catania, Italy*

[4]*Centre for Quantum Technologies, National University of Singapore, 3 Science Drive 2, Singapore 117543, Singapore*

[5]*MajuLab, CNRS-UNS-NUS-NTU International Joint Research Unit, UMI 3654, Singapore*

[6]*CNR-IMM & INFN-Sezione di Catania, Via S. Sofia 64, I-95127 Catania, Italy*

[7]*LANEF* 'Chaire d'excellence', *Université Grenoble-Alpes & CNRS, F-38000 Grenoble, France*

(Received 17 November 2019; accepted 13 March 2020; published 27 April 2020)

We study the ground state of two interacting bosonic particles confined in a ring-shaped lattice potential and subjected to a synthetic magnetic flux. The system is described by the Bose-Hubbard model and solved exactly through a plane-wave Ansatz of the wave function. We obtain energies and correlation functions of the system both for repulsive and attractive interactions. In contrast with the one-dimensional continuous theory described by the Lieb-Liniger model, in the lattice case we prove that the center of mass of the two particles is coupled with its relative coordinate. Distinctive features clearly emerge in the persistent current of the system. While for repulsive bosons the persistent current displays a periodicity given by the standard flux quantum for any interaction strength, in the attractive case the flux quantum becomes fractionalized in a manner that depends on the interaction. We also study the density after a long time expansion of the system. Our results can be used to benchmark approximate schemes for the many-body problem such as the density matrix renormalization group or other variational schemes.

DOI: 10.1103/PhysRevA.101.043418

I. INTRODUCTION

Bosonic particles confined in a ring geometry can be realized with different quantum technological platforms, ranging from superconducting circuits [1] to circuit quantum electrodynamics (QED) [2], and to cold atoms [3–8]. There are many reasons explaining the relevance of such systems for the physics community. First, the periodic boundary conditions provide a textbook route to emulate quantum systems with strict translational symmetry and to simplify the access to the large number of particles (N) regime of the system (thermodynamic limit) [9]. On the other hand, systems with closed spatial architectures provide the simplest instance of quantum circuits that are able to sustain nontrivial current states that can be used in quantum technology to construct quantum devices and quantum sensors with enhanced performances [10,11]. Here, we focus on the persistent currents, which are bosonic current states originating from the coherence of the system [12–15]. Such specific current states of thermodynamic nature can be imparted to the bosons by a real or synthetic magnetic field [16]. Persistent currents have been of defining importance in mesoscopic physics [17]. Recently, persistent currents have been attracting upsurged interest, especially in the cold-atom community as they grant an enhanced flexibility and control over the physical conditions of the system [18–33].

Bose statistics enables a multiparticle interaction that can make interacting bosonic systems difficult to handle. In this respect, it is instructive to consider the interplay between the Bose gas field theory (pointlike interaction) and the Bose-Hubbard model, providing two celebrated schemes describing many-body bosonic theories. The homogeneous Bose gas in one spatial dimension, described by the Lieb-Liniger model, is a continuous field theory that is integrable by Bethe Ansatz: The many-body scattering can be factorized in two-particle scatterings where the scattering is "nondiffractive" [34]. In contrast, the Bose-Hubbard model, introduced by Haldane as a lattice regularization of the Bose-gas field theory, is not integrable and the scattering is diffractive [35–37]. The two theories are equivalent in a dilute limit of very few particles per lattice site. In such a limit, in which multiple occupancy is loosely speaking demoted, the Bose-Hubbard dynamics becomes integrable. Such considerations can be expressed quantitatively through coordinate Bethe Ansatz. Indeed, it was demonstrated that the Bose-Hubbard model cannot be solved by coordinate Bethe Ansatz if there exists a probability of having more than two particles at the same site [36]. Thus, the two-particle Bose-Hubbard model is analytically accessible. Despite the simplicity of the system, the $N = 2$ Bose-Hubbard model (2BHM) has been demonstrated to provide a very useful case study to decode some of the general features of the many-body theory. Recently, the 2BHM has been employed to answer relevant questions concerning cold atoms confined in optical lattices [38–41]. Dynamical effects of bosonic pairs in a one-dimensional lattice, both in the attractive and repulsive case, have been also analyzed [42].

In this work, we will employ the 2BHM to the persistent currents in a ring-shaped lattice potential by exact means.

*juan.polo@oist.jp

To this end, we use the exact expression of the two-body wave function in the presence of an external gauge field. We calculate relevant observables and correlation functions characterizing the system. We discuss the differences between our results and those coming from the continuous Bose gas field theory.

The article is outlined as follows: in Sec. II, we present the model system together with the expressions for the exact spectrum and correlation functions, in Secs. III and IV, we discuss the results for positive and negative interactions, respectively, and finally in Sec. V, we draw our conclusions.

II. MODEL SYSTEM AND OBSERVABLES

We model the system of interacting bosons trapped in a L-site lattice ring under the presence of the synthetic gauge field using the Bose Hubbard model:

$$\begin{aligned} H(\Omega, U) &= K(\Omega) + V(U), \\ K(\Omega) &= -J_0 \sum_{j=1}^{L} (e^{i2\pi\Omega/L}\, b_j^\dagger b_{j+1} + \text{H.c.}), \\ V(U) &= +\frac{U}{2} \sum_{j=1}^{L} n_j(n_j - 1), \end{aligned} \tag{1}$$

where b_j is the bosonic annihilation operator and $n_j = b_j^\dagger b_j$ is the local number operator for the site j. The parameters U and J_0 account for the strength of the on-site interactions and tunneling amplitude, respectively, and Ω is a synthetic gauge field that can be generated in different ways [16,43], for example, stirring the condensate on a ring of radius $R = La/2\pi$, with a the lattice spacing. Here, the effect of the synthetic field is taken into account through the Peierls substitution leading to the exponential term in Eq. (1) (see Appendix A for a more detailed derivation). We assume that the size of the system is sufficiently large such that the Peierls substitution becomes well defined [44].

In the next sections, we will discuss the properties of the system for both positive and negative interactions U. Since $V(-U) = -V(U)$ and $\mathcal{K}(\Omega) = -\mathcal{K}(\Omega + L/2)$, the following symmetries connect the two cases:

$$H(\Omega, U) = K(\Omega + L/2) - V(-U) \tag{2}$$

$$= -H(\Omega + L/2, -U); \tag{3}$$

in addition,

$$H(\Omega, U) = -H(\Omega, -U). \tag{4}$$

The current operator, which is the most relevant observable to describe persistent currents, in dimensionless units reads

$$I(\Omega) \equiv -\frac{\partial \hat{H}}{\partial \Omega} = i\frac{2\pi J_0}{L} \sum_j (e^{2\pi i\Omega/L} b_j^\dagger b_{j+1} - \text{H.c.}). \tag{5}$$

The persistent current can also be obtained through thermodynamic potentials and, in particular, at zero temperature it is given by

$$\langle I(\Omega)\rangle = -\frac{\partial E}{\partial \Omega}, \tag{6}$$

where E is the ground-state energy of the system.

A classic result in the field was obtained by Leggett [45]. By resorting to the analogy of particles moving in a magnetic field and using the Bloch theorem for particles in a periodic potential, it can be demonstrated that the energy of the many-body system displays a periodicity in Ω that is fixed by the elementary flux quantum of the system. Therefore, due to Eq. (6), the persistent current is also a periodic function of Ω with the same periodicity. This result holds for any local two-body interaction that allows for a center-of-mass and relative coordinate decoupling [45]. In the next sections, the Leggett results will be analyzed for the 2BHM.

In the limit of small filling fractions $\nu = N/L = D\Delta$, with $D = N/(L\Delta)$ being the density and Δ being the lattice spacing, the one-dimensional Bose-Hubbard model can be mapped into the integrable Bose gas field theory or, in first quantization, the Lieb-Liniger model [46,47]. The latter describes a continuum model of bosons of mass m in one dimension with contact delta interactions $v(x - x') = g\delta(x - x')$. Note that for our particular purposes, we consider a superfluid regime (un-commensurate N/L). In particular, here we keep the dimensionless coupling strength of the Lieb-Liniger model, $\gamma = mg/\hbar^2 D$ constant.

The parameters of the lattice and continuous theories are related by $U = g/\Delta$ and $J_0 = \hbar^2/2m\Delta^2$, yielding $\gamma = \nu^{-1}(U/J_0)$. Hence, by increasing the number of lattice sites L at fixed particle number N, the interaction to the tunnel energy ratio U/J_0 should be decreased in order for the Bose gas limit to be achieved. We note that, since the continuous rotational symmetry of the Lieb-Liniger model is reduced to a discrete one, in the lattice the current operator is generically distinct from the angular momentum. In particular, $I(\Omega)$ in Eq. (5) does not commute with the Hamiltonian in Eq. (1) [interaction term $V(U)$]. In a dynamical protocol, therefore, the current would not be conserved [48]. Nevertheless, $\langle I(\Omega)\rangle$ will be denoted as the "persistent current" in analogy of the current states of the continuous theory (see also [49]). Important insights on the current states of the system can be obtained by the current's fluctuations,

$$\Delta I(\Omega) = \sqrt{\langle I(\Omega)^2\rangle - \langle I(\Omega)\rangle^2}. \tag{7}$$

In cold-atom settings, the current state manifests itself in the time-of-flight expansion (TOF) images, i.e., the particle density after the condensate is released from the confining potential. The long time density pattern can be calculated through the momentum distribution at the instant at which the trap is opened, according to

$$n(\mathbf{k}) = |w(\mathbf{k})|^2 \sum_{j,l} e^{i\mathbf{k}\cdot(\mathbf{x}_j - \mathbf{x}_l)} \langle b_j^\dagger b_l\rangle, \tag{8}$$

where $\mathbf{x}_j$ is the position of the lattice sites in the plane of the ring and $w(\mathbf{k})$ are the Fourier transforms of the Wannier functions.

In the following, we will obtain exact expressions both for the spectrum and correlation functions of the 2BHM, granting us access to the relevant observables describing the persistent currents of the system.

The Bose-Hubbard model in the two-particle sector

While not true for general N, the Bose-Hubbard model in the $N = 2$ sector is exactly solvable *à la* coordinate Bethe

Ansatz [42]. As we shall see, this approach allows us to deal with the persistent current of the system exactly, in the case in which the ring is exposed to an effective magnetic field. A general two-boson state can be written as

$$|\phi\rangle = \sum_{j,k=1}^{L} \phi_{jk} \hat{b}_j^\dagger \hat{b}_k^\dagger |0\rangle, \tag{9}$$

with the two-particle coefficients ϕ_{jk} being symmetric under the exchange of j and k and normalized such that $\langle\phi|\phi\rangle = 1$. The Schrödinger equation $H|\phi\rangle = E|\phi\rangle$ reads

$$F_{jk} = (E - U\delta_{jk})\phi_{jk}, \tag{10}$$

where it is given by $F_{jk} \doteq -J(\phi_{j+1,k} + \phi_{j,k+1}) - J^*(\phi_{j-1,k} + \phi_{j,k-1})$.

The solution of Eq. (10) is obtained with a plane-wave Ansatz for ϕ_{jk}, which is certainly correct in the noninteracting limit $U = 0$ [50]:

$$\begin{aligned}\phi_{jk} = &[a_{12}e^{i(p_1 j + p_2 k)} + a_{21}e^{i(p_1 k + p_2 j)}]\vartheta(j-k) \\ &+ [a_{12}e^{i(p_1 k + p_2 j)} + a_{21}e^{i(p_1 j + p_2 k)}]\vartheta(k-j),\end{aligned} \tag{11}$$

where p_i are the wave vectors of each particle, where wave vectors and the coordinate are for simplicity written in units of $1/a$ and a, respectively, and $\vartheta(x)$ corresponds to the Heaviside step function.

Equation (10) for $j \neq k$ is solved using

$$\begin{aligned}E &= \langle\phi|\hat{H}|\phi\rangle = -2J_0(\cos p_1 + \cos p_2) \\ &= -4J_0 \cos\left(\frac{P}{2} + \frac{2\pi\Omega}{L}\right)\cos(p),\end{aligned} \tag{12}$$

where we introduced the center-of-mass and relative coordinates for both space and momentum coordinates:

$$X = \frac{j+k}{2} \qquad x = j - k, \tag{13}$$

$$P = p_1 + p_2 \qquad p = \frac{p_1 - p_2}{2}. \tag{14}$$

This allows us to rewrite Eq. (11) as

$$\phi_{Xx} = a_{12}e^{iPX}\left(e^{ip|x|} + \frac{a_{21}}{a_{12}}e^{-ip|x|}\right). \tag{15}$$

The plane-wave Ansatz (11) is exact also for interacting particles since for $U \neq 0$ the effect of the interaction can be recasted into the scattering between the two sectors, $j > k$ and $j < k$, in which the particles are noninteracting. Indeed, by introducing (15) into Eq. (10) for $j = k$, the ratio between the coefficients, $y(P, p) \doteq \frac{a_{21}}{a_{12}}$, can be obtained as a phase shift of the wave function:

$$y(P,p) = -\frac{\frac{U}{4J_0} - i\cos\left(\frac{P}{2} - \frac{2\pi\Omega}{L}\right)\sin(p) - 2\cos(p)\sin\left(\frac{P}{2} - \frac{\pi\Omega}{L}\right)\sin\left(\frac{\pi\Omega}{L}\right)}{\frac{U}{4J_0} + i\cos\left(\frac{P}{2} - \frac{2\pi\Omega}{L}\right)\sin(p) - 2\cos(p)\sin\left(\frac{P}{2} - \frac{\pi\Omega}{L}\right)\sin\left(\frac{\pi\Omega}{L}\right)}, \quad |y(P,p)| = 1. \tag{16}$$

The allowed values of the momenta are fixed by the boundary conditions. If not otherwise stated, we assume periodic boundary conditions,

$$\phi_{j,1} = \phi_{j,L+1}, \tag{17}$$

leading to the following equations for the center of mass and relative momenta:

$$P_n = \frac{2\pi n}{L}; \quad (-1)^n e^{ipL} = y(P_n, p), \tag{18}$$

with $n = \{1, \cdots, L\}$. Note that in a finite ring the center-of-mass momentum takes discrete values, therefore we explicitly show that using the subscript n.

The relative momentum p depends on U/J_0 and Ω explicitly, and can be either real or complex valued giving rise to *scattering* or *bound* states, respectively. With the chosen periodic boundary conditions, the center-of-mass momentum P does not depend directly on Ω or on U/J. Alternatively, with the twisted boundary conditions $\phi_{j,1} = e^{i\Omega}\phi_{j,L+1}$, Ω can be gauged away from the scattering matrix. In this case, Ω would have shifted the center of mass P (see Appendix B).

Correlation functions. In the following we calculate the one-body (two-point) and two-body (four-point) correlations that are needed to map out the observables of the system. The two-point correlation function is

$$C_r^{1b} = \langle b_l^\dagger b_{l+r}\rangle = \sum_m \phi_{l,m}^* \phi_{m,l+r}. \tag{19}$$

Resorting to the translational invariance of the system, we can set $l = 0$ and $m > 0$. We obtain

$$\begin{aligned}C_r^{1b} = 2\mathcal{N}^2 e^{iP\frac{r}{2}}\Big[&\frac{1}{2}\csc(p)(\sin(p(L+r+1)-\psi) \\ &+ \sin(p(L-r-1)-\psi) - \sin(p(1+r)-\psi) \\ &+ \sin(p(1-r)+\psi) + \sin(p+pr) - \sin(p-pr)) \\ &+ (L-r)\cos(pr) + r\cos(pr-\psi)\Big],\end{aligned} \tag{20}$$

where $\psi \doteq \xi_{12} - \xi_{21}$ with $\xi_{i,j}$ given by $a_{12} = \mathcal{N}e^{-i\xi_{12}}$ and $a_{21} = \mathcal{N}e^{-i\xi_{21}}$ (note that, by construction, $|a_{21}/a_{12}|^2 = 1$).

The density-density correlations $\langle n_l n_{l+r}\rangle$ are

$$\begin{aligned}C_r^d &= \langle n_l n_{l+r}\rangle = |\phi_{l,l+r}|^2 \\ &= 2\mathcal{N}^2[1 + \mathrm{Re}(e^{i\psi - 2ipr})].\end{aligned} \tag{21}$$

The connected correlation, $\langle n_l n_{l+r}\rangle - \langle n_0 n_0\rangle$, can be calculated by subtracting $(N/L)^2$ from the density-density correlation (21).

Both C_r^{1b} and C_r^d depend on p explicitly. Therefore, the actual behavior of such quantities is substantially affected by whether the particles are attractive or repulsive.

For attractive interactions, the lowest energy eigenstate for each center-of-mass wave vector has a complex-valued relative momentum, such that $p = i\alpha$, which leads to an

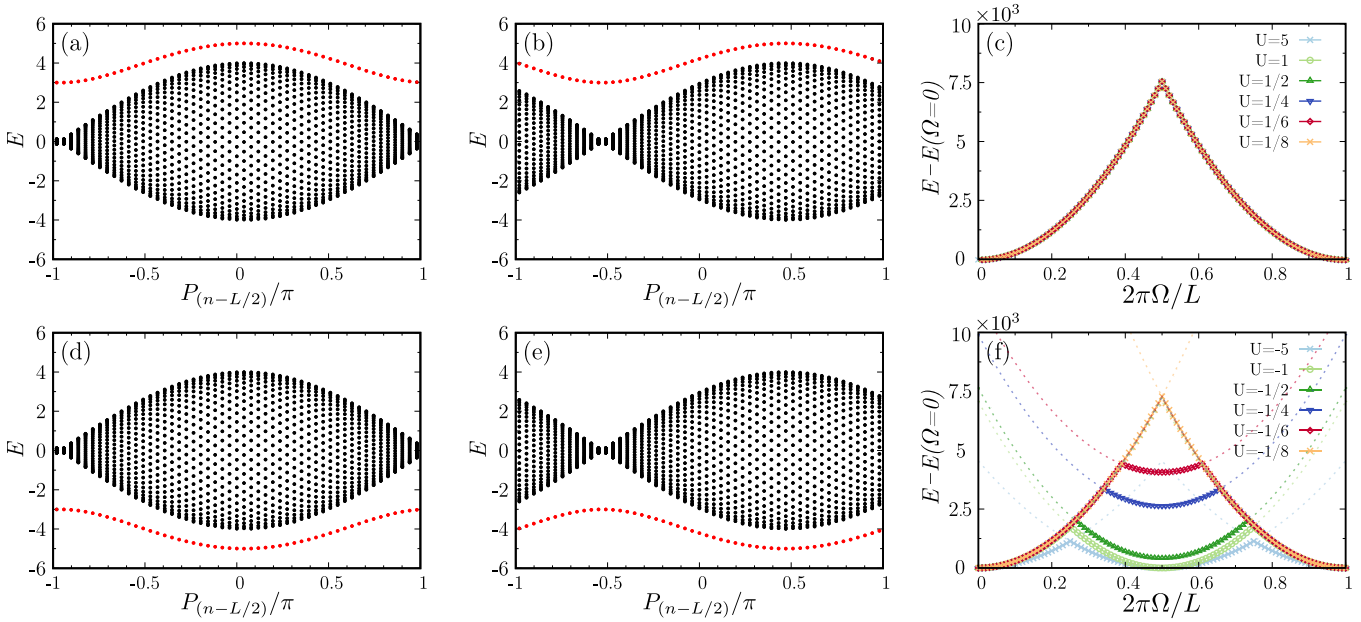

FIG. 1. Energy spectrum of the model for a ring lattice of $L = 51$ sites in units of J_0. (a) and (b) $U = 5$ (first row); (d) and (e) $U = -5$ (second row). In panels (a) and (d) the flux is set to $2\pi\Omega/L = 0.5$ while in panels (b) and (e) it is set to $2\pi\Omega/L = 0.25L$. In panels (c) and (f) we plot the energy of the ground state as a function of the flux, shifted by its value at $\Omega = 0$ and rescaled by a factor of 10^3, for different values of the interaction strength as indicated in the figure. (f) Also shown is each corresponding first excited state using a dashed line.

exponential decay in the correlation functions:

$$C_r^{d,\mathrm{BOUND}} = 2\mathcal{N}^2[1 + e^{-2\alpha r}\cos(\psi)]. \tag{22}$$

We define the scale at which the correlations decay as $\xi = 1/\alpha$. This quantity defines the characteristic length of the bound state.

Finally, we calculate the pair correlation function:

$$\begin{aligned} C^p_{l,j} &= \langle b_l^\dagger b_l^\dagger b_j b_j\rangle = \phi^*_{l,l}\phi_{j,j} \\ &= 2\mathcal{N}^2(\cos(rP/2) - i\sin(rP/2)). \end{aligned} \tag{23}$$

We note that this quantity does not depend on p and therefore does not distinguish between bound and scattering states.

III. RESULTS FOR REPULSIVE INTERACTIONS

In this section we obtain the exact spectrum of the Hamiltonian and the persistent currents for positive U, thus generalizing the results obtained in Ref. [42] at $\Omega = 0$.

A. Energy spectrum

We start by analyzing the spectrum and the ground-state energy of the system. We note that there are two main bands in the system [see Figs. 1(a) and 1(b)]. The lowest band is characterized by real rapidities and therefore corresponds to scattering states. On top of it, we find a distinct band of bound states with complex rapidities. The two bands are separated by a finite gap, formed by the energy eigenstates with the largest energy eigenvalue for each center-of-mass momentum P_n. Figure 1(c) shows the ground-state energy of the system as a function of the induced flux Ω. Note that the interactions change the ground state independently of the magnetic field [42].

B. Persistent currents

The ground-state persistent current displays the characteristic sawtooth dependence on the synthetic magnetic field. The jumps of the persistent currents (from clockwise to anticlockwise) and the slope of the sawtooth are determined by the flux quantum of the system [45]. In the repulsive case, the current jumps occur at values that are independent of the particle number and interaction strength [see Fig. 2(a)]. Moreover, the slopes of the sawtooth behavior of the current are also independent of the interaction U. This scenario indicates that the flux quantum is a fixed quantity (independent of N and U).

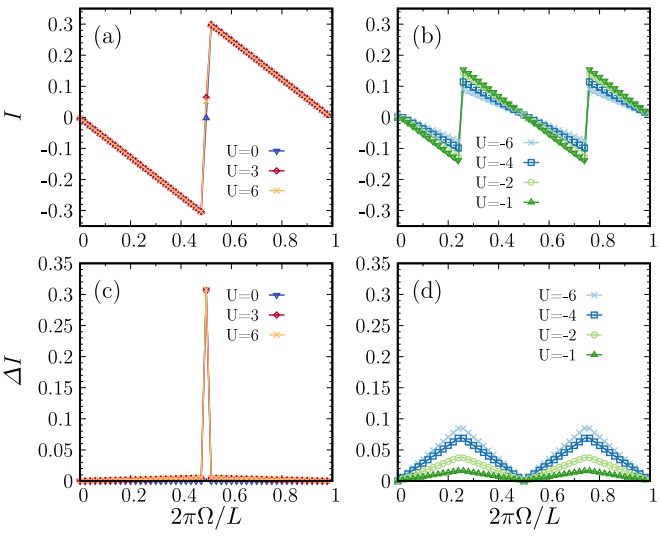

FIG. 2. Current (upper row) and its fluctuations (lower row) as a function of Ω for different values of the interaction strength in dimensionless units [see Eqs. (5) and (7)]. (Left panels) Repulsive interactions. (Right panels) Attractive interactions.

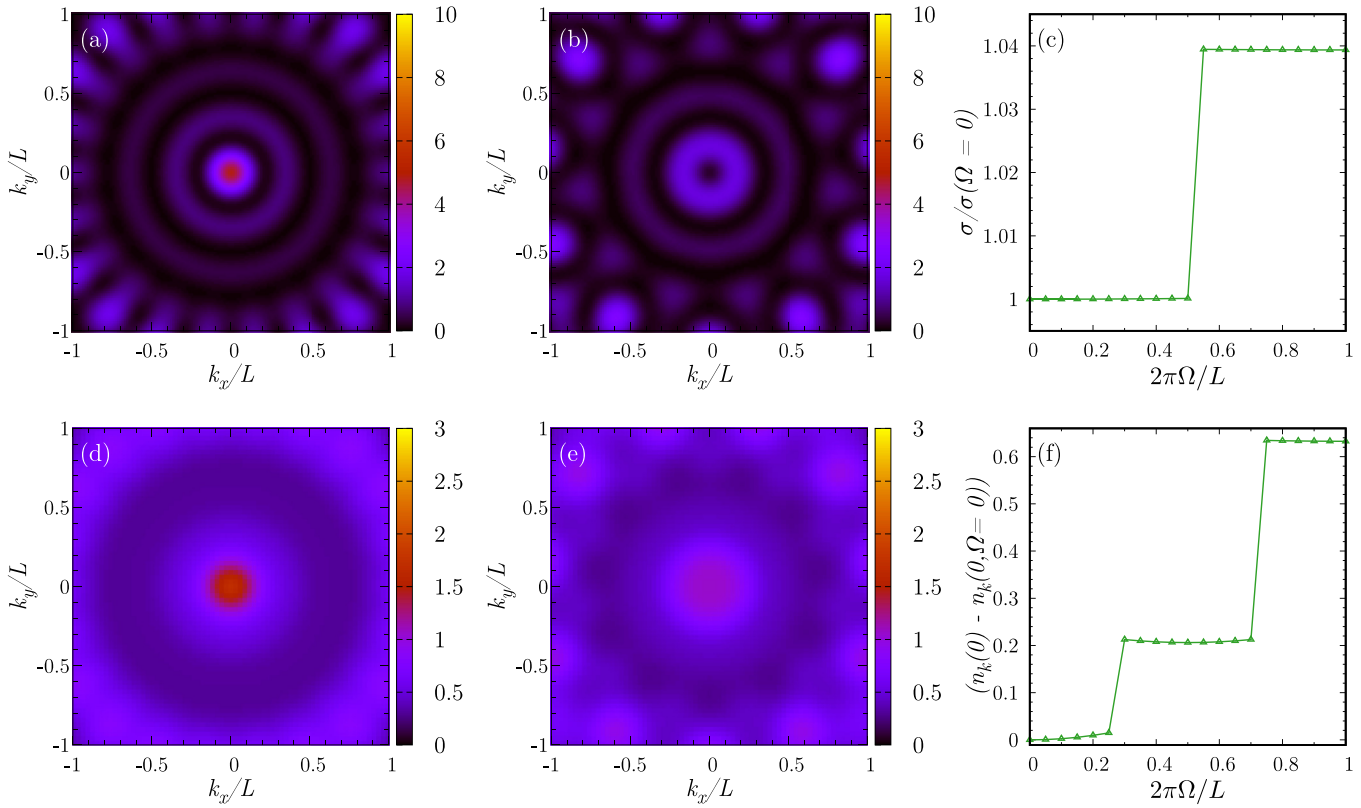

FIG. 3. Time-of-flight density plots are displayed in (a), (b), (d), and (e) for a chain of $L = 11$ sites. (c) and (f) The TOF central peak width σ, and the TOF central value $n_k(\mathbf{k} = 0)$, respectively. Top panels show the repulsively interacting case with $U = 5$ and lower panels the attractively interacting one with $U = -5$. Density plots correspond to (a) $\Omega = 0.0$, (b) $\Omega = 0.8$, (d) $\Omega = 0.0$, and (e) $\Omega = 0.8$. To highlight the TOF features we set $|w(\mathbf{k})|^2 = 1$ in (a) and (b) and (d) and (e). The dispersion of the interference pattern (c), with $\sigma^2 = \int d\mathbf{k}\, \mathbf{k}^2 n(\mathbf{k})$, is calculated with the rescaled Wannier function $|w(\mathbf{k})|^2 = \exp((k_x^2 + k_y^2)/(L/2)^2)$ and it is normalized by $\sigma(\Omega = 0)$.

At $2\pi\Omega/L = 1/2$ where the jump in the current occurs, the fluctuation ΔI reaches its maximum value. Note that at this particular point the ground state of the system will be degenerate with the first excited state [45] and thus, the current state is no longer a well-defined one, or in other words it does not possess a good associated quantum number. Therefore, a frequency of $2\pi\Omega/L = 1/2$ is the ideal candidate to create a superposition among two current states, corresponding to the $0 - th$ and $1 - st$ energy minima, which can be achieved by an infinitesimal perturbation breaking the rotation symmetry that would open the degeneracy point.

The current states in the system arise in the long-time expansion of the density of the cold-atom gas after releasing the confining potential. For $\Omega = 0$, the interference pattern displays a marked peak at $\mathbf{k} = 0$. For Ω larger than the first degeneracy point in the ground-state energy, $\langle n_{\mathbf{k}}(\mathbf{0})\rangle$ is depressed, with a characteristic ring-shape symmetry [see Figs. 3(a)–3(c)]. It has been demonstrated that the radius of such a ring-shape feature in the expansion increases with Ω in quantized steps [51] thus, we calculate the TOF dispersion $\sigma^2 = \int d\mathbf{k}\, \mathbf{k}^2 n(\mathbf{k})$ to characterize such a characteristic increase [see Fig. 3(c)].

IV. RESULTS FOR ATTRACTIVE INTERACTIONS

In this section we consider the case $U < 0$ and present the excitation spectrum and the ground-state persistent current as a function the frequency Ω.

A. Energy spectrum

We first focus on the energy spectrum of the two-particle system [see Figs. 1(d) and 1(e)]. The results at $\Omega = 0$, are in agreement with the N-particle case obtained through the study of the dynamical structure factor [52].

For nonzero Ω the spectrum is displaced, with a maximum displacement given by the maximum momentum allowed by the lattice. This is due to the specific coupling between the center of mass and rotation. In Fig. 1(d) we show the spectrum for attractively interacting bosons at a rotation frequency $2\pi\Omega/L = 1/2$, corresponding to half of the periodicity expected for noninteracting or repulsively interacting particles. For completeness, in Fig. 1(e) we show an example where a large momenta $2\pi\Omega/L = L/4$ is induced, which corresponds to a quarter of the maximum angular momenta allowed by the periodicity imposed by the lattice. In addition, Ω changes the magnitude of the relative momenta, which is directly related to the characteristics of the bound states, e.g., the decay length in the density-density correlation function. In our lattice system, this coupling between the relative and center-of-mass momenta (disappearing in the continuous Lieb-Lineger case) has substantial implications on the dynamics of the system.

A doubling of the periodicity occurs in the lowest energy brand of the spectrum. This behavior, that should be contrasted with the repulsive case, has clear implications on the periodicity of the persistent current [53].

Figure 1(e) shows the ground-state energy of the system as a function of the frequency of rotation. Note that the change of parabola corresponds to the degeneracy point between the two lowest energy eigenstates of the system. Contrary to the predictions of the Lieb-Liniger model, the doubling of periodicity in the lattice does depend on the strength of the interactions.

B. Persistent current

For attractive interactions, the ground-state persistent current also displays the characteristic sawtooth dependence on the effective magnetic field [31,45]. Compared with the positive U case, the persistent current exhibits a fine structure. In fact, it has been recently shown through numerical simulations of the attractive BHM that the current has a N periodicity dependence [53]. In addition, the slope of the sawtooth depends on U. This scenario implies that the flux quantum is reduced by bound states in which more particles can share the same amount of magnetic flux [see Fig. 2(b)], indicating fractionalization of angular momentum per particle [53]. In this case, the composition of the bound states is a variable quantity depending on the interaction. As a consequence, the response to the magnetic field can be different for different interactions.

For attractive interactions, the current fluctuations follow the Ω periodicity of the current. In comparison with the repulsive case, $\Delta I(\Omega)$ are much more pronounced. Such a distinctive feature is an expression of the different impact that the nonconservation of current has for repulsive and attractive interaction: Going from positive to negative U, multiple occupancy of the lattice sites is more and more probable and therefore the effect of the current's nonconservation increases accordingly.

Because of the different nature of coherence of attracting bosons, the TOF interference fringes display marked differences from those obtained in the repulsive case. For both $\Omega = 0$ and $\Omega \neq 0$, we observe a broad peak centered around $\mathbf{k} = 0$. Remarkably, the information on the current states is still encoded in the TOF as shown in Figs. 3(d)–3(f). In particular, in Fig. 3(f) we calculate the central peak $n_k(\mathbf{k} = 0)$, which displays clear jumps between different plateaus, directly showing the fractionalization of the angular momentum.

V. CONCLUSIONS

In this paper we study the exact ground-state properties of the Bose-Hubbard model for two interacting bosons moving in a ring-shaped potential pierced by an effective magnetic field. In this case, the wave function can be expressed as a suitable combination of plane waves *á la* coordinate Bethe Ansatz. Our analysis shows that the interaction can couple the center of mass of the particles and their relative coordinate. This characteristic trait of the lattice system, that is lost in the continuous (integrable) Bose gas or Lieb-Lineger theory, leads to striking consequences in the structure of the ground state, particularly for attractive interactions. In the language of the Bethe Ansatz, while for repulsive interactions the ground state of the system is made of scattering states with real rapidities, for negative U the ground state is a bound state with complex rapidities with a two-string structure. In the latter case, it was demonstrated that the bound states describe the quantum analog of bright solitons [52]. We note that for sufficiently large interactions these bound states are protected by a finite energy gap. This feature is lost in the continuous case.

We note that the center-of-mass and relative coordinate coupling has mild consequences on the persistent current for repulsive interactions indicating that the two coordinates cannot be resolved in scattering states. In the case of attractive interactions, instead, the Ω periodicity of the ground-state energy and therefore the Ω dependence of the persistent current is affected by the total number of particles, i.e., doubled in this case (the general N dependence has been studied in [53]). This effect is a manifestation of the formation of a composite particle made out of two bosons. Because of the nontrivial dynamics of the relative coordinate, a more subtle effect emerges. Indeed, the Ω periodicity of the ground-state energy does depend on the interaction. This scenario indicates that the aforementioned composite object can respond as a particle with a variable mass depending on the interaction. Therefore, the flux quantum for attractive bosons is also a variable quantity that depends on the interaction.

In a cold-atom setting, such effects are visible through the time-of-flight expansion of the condensate $\langle n(\mathbf{k})\rangle$. While the current state in repulsive bosons displays the characteristic ring-shape suppression of the density at $\mathbf{k} = 0$ in $\langle n(\mathbf{k})\rangle$, the persistent current of attractive bosons remains peaked at $\mathbf{k} = 0$. Despite the seemingly featureless interference, the flux quantum fractionalization emerges as a quantized dispersion of the fringe around the peak at $\mathbf{k} = 0$.

Our results can be used as a benchmark for numerical or other approximated schemes for the many-body problem. In particular, it would be interesting to study how the structure of the ground state is modified by the departure from the integrability.

ACKNOWLEDGMENTS

We thank V. Dunjko, M. Olshanii, and H. Perrin for discussions. The Grenoble LANEF framework (ANR-10-LABX-51-01) is acknowledged for its support with mutualized infrastructure. We also acknowledge financial support from the ANR project SuperRing (Grant No. ANR-15-CE30-0012).

APPENDIX A: SYNTHETIC GAUGE FIELD

Synthetic gauge fields can be generated in different ways [16,43]. Here, we summarize how synthetic gauge fields can be induced by stirring the condensate. The rotation of the condensate can be induced by a time-dependent potential $V(x-\Omega t)$ moving at an angular velocity Ω_r on a ring of radius R. The time-dependent Hamiltonian is

$$\mathcal{H}(\Omega, t) = \mathcal{H}_0 + V(x-\Omega R t), \tag{A1}$$

where $\mathcal{H}_0 = \sum_{l=0}^{N} -\frac{\hbar^2}{2m}\nabla_l^2 + \hat{U}_{\rm int}$, is expressed by the sum of the kinetic energy and a potential term describing the atom-atom interactions $\hat{U}_{\rm int}$. In the following, we assume that $\hat{U}_{\rm int} = U\sum_{l,m}\delta(\mathbf{x}_l - \mathbf{x}_m)$. By changing to the rotating reference frame with the same frequency Ω_r as the external

potential, the Hamiltonian is not time dependent:

$$\mathcal{H}_{\rm rot} = \mathcal{U}^\dagger(t)\,\mathcal{H}(\Omega,t)\,\mathcal{U}(t) = \mathcal{H}_0 + V(x) - \Omega_r L_z, \quad \text{(A2)}$$

where $\mathcal{U}(t) = \exp[iL_z\Omega_r t/\hbar]$, and L_z is the z-component angular momentum operator, with z being the coordinate perpendicular to the plane of the ring.

In the second quantization, the Hamiltonian above reads

$$H = \int d\mathbf{x}\Psi^\dagger(\mathbf{x})\mathcal{H}_{\rm rot}\Psi(\mathbf{x}), \quad \text{(A3)}$$

where $\Psi(\mathbf{x})$ are bosonic field operators. Using the standard procedure of completing the squares in the kinetic terms, the Hamiltonian reads

$$H = \int d\mathbf{x}\Psi^\dagger(\mathbf{x})\left(\sum_{l=0}^{N}\frac{(-i\hbar\nabla_l + A)^2}{2m} - \frac{A^2}{2m} + V_p\right)\Psi(\mathbf{x}), \quad \text{(A4)}$$

where $\vec{A} = R\vec{L}_z$ is the effective vector potential and we define $V_p = +U_{\rm int} + V(x)$.

In a lattice system, the field operators can be expanded in Wannier functions: $\Psi(\mathbf{x}) = \sum_l w_l(\mathbf{x})a_l$, being a_l the site l annihilation bosonic operator. Therefore:

$$H = \sum_{l,m}\int d\mathbf{x} w_l(\mathbf{x}) \times\left[\frac{(-i\hbar\sum_l\nabla_l + A)^2}{2m} - \frac{A^2}{2m} + V_p\right]w_m(\mathbf{x})a_l^\dagger a_m. \quad \text{(A5)}$$

The vector potential can be gauged away by redefining the Wannier functions: $\tilde{w}_l(\mathbf{x}) = w_l(\mathbf{x})e^{iA\mathbf{x}_l}$. This procedure, known as Peierls substitution, leads to our Hamiltonian in Eq. (1) with $\Omega = \Omega_r/(\hbar/mR)$.

APPENDIX B: TWISTED BOUNDARY CONDITIONS

By performing a unitary transformation of the Hamiltonian given in Eq. (1), in this case a *rotation* $U = e^{2\pi i\Omega}$, we change from periodic boundary conditions to twisted boundary conditions [54,55]. Such transformation simplifies the system Hamiltonian to the one obtained for a nonrotating system, i.e., with real tunneling amplitudes. Moreover, we also obtain simplified equations for the energy, center of mass, and relative momenta which now read

$$E^{\rm TB} = -4J\cos\left(\frac{P^{\rm TB}}{2}\right)\cos(p^{\rm TB}), \quad \text{(B1)}$$

$$P_n^{\rm TB} = \frac{2\pi}{L}(n - 2\Omega), \quad \text{(B2)}$$

$$(-1)^n e^{ip^{\rm TB}L} = y^{\rm TB}\left(P_n^{\rm TB}, p^{\rm TB}\right), \quad \text{(B3)}$$

with

$$y^{\rm TB}(P,p) = \frac{U - i4J\cos\left(\frac{P}{2}\right)\sin(p)}{U + i4J\cos\left(\frac{P}{2}\right)\sin(p)}. \quad \text{(B4)}$$

Note that in the previous equations, the induced rotation determined by the frequency Ω only appears explicitly in the center-of-mass coordinate. Nonetheless, both center-of-mass and relative coordinates are still coupled as can be seen through the continuity of the energy and implicitly though $y^{\rm TB}(P,p)$.

[1] P. Krantz, M. Kjaergaard, F. Yan, T. P. Orlando, S. Gustavsson, and W. D. Oliver, Appl. Phys. Rev. **6**, 021318 (2019).

[2] A. Blais, J. Gambetta, A. Wallraff, D. I. Schuster, S. M. Girvin, M. H. Devoret, and R. J. Schoelkopf, Phys. Rev. A **75**, 032329 (2007).

[3] O. Morizot, Y. Colombe, V. Lorent, H. Perrin, and B. M. Garraway, Phys. Rev. A **74**, 023617 (2006).

[4] S. Franke-Arnold, J. Leach, M. J. Padgett, V. E. Lembessis, D. Ellinas, A. J. Wright, J. M. Girkin, P. Öhberg, and A. S. Arnold, Opt. Express **15**, 8619 (2007).

[5] K. C. Wright, R. B. Blakestad, C. J. Lobb, W. D. Phillips, and G. K. Campbell, Phys. Rev. Lett. **110**, 025302 (2013).

[6] G. Gauthier, I. Lenton, N. M. Parry, M. Baker, M. J. Davis, H. Rubinsztein-Dunlop, and T. W. Neely, Optica **3**, 1136 (2016).

[7] C. Muldoon, L. Brandt, J. Dong, D. Stuart, E. Brainis, M. Himsworth, and A. Kuhn, New J. Phys. **14**, 073051 (2012).

[8] K. Henderson, C. Ryu, C. MacCormick, and M. G. Boshier, New J. Phys. **11**, 043030 (2009).

[9] M. E. Fisher and M. N. Barber, Phys. Rev. Lett. **28**, 1516 (1972).

[10] A. Acín, I. Bloch, H. Buhrman, T. Calarco, C. Eichler, J. Eisert, D. Esteve, N. Gisin, S. J. Glaser, F. Jelezko, S. Kuhr, M. Lewenstein, M. F. Riedel, P. O. Schmidt, R. Thew, A. Wallraff, I. Walmsley, and F. K. Wilhelm, New J. Phys. **20**, 080201 (2018).

[11] S. Ragole and J. M. Taylor, Phys. Rev. Lett. **117**, 203002 (2016).

[12] V. Ambegaokar and U. Eckern, Phys. Rev. Lett. **65**, 381 (1990).

[13] M. Büttiker, Y. Imry, and R. Landauer, Phys. Lett. A **96**, 365 (1983).

[14] L. P. Lévy, G. Dolan, J. Dunsmuir, and H. Bouchiat, Phys. Rev. Lett. **64**, 2074 (1990).

[15] N. O. Birge, Science **326**, 244 (2009).

[16] J. Dalibard, F. Gerbier, G. Juzeliūnas, and P. Öhberg, Rev. Mod. Phys. **83**, 1523 (2011).

[17] Y. Imry, *Introduction to Mesoscopic Physics*, 2 (Oxford University Press, USA, 2002).

[18] A. R. Kolovsky, New J. Phys. **8**, 197 (2006).

[19] M. Maik, P. Buonsante, A. Vezzani, and J. Zakrzewski, Phys. Rev. A **84**, 053615 (2011).

[20] P. Vaity and R. P. Singh, Opt. Lett. **36**, 2994 (2011).

[21] A. Ramanathan, K. C. Wright, S. R. Muniz, M. Zelan, W. T. Hill, C. J. Lobb, K. Helmerson, W. D. Phillips, and G. K. Campbell, Phys. Rev. Lett. **106**, 130401 (2011).

[22] C. Ryu, P. W. Blackburn, A. A. Blinova, and M. G. Boshier, Phys. Rev. Lett. **111**, 205301 (2013).

[23] S. Eckel, J. G. Lee, F. Jendrzejewski, N. Murray, C. W. Clark, C. J. Lobb, W. D. Phillips, M. Edwards, and G. K. Campbell, Nature (London) **506**, 200 (2014).
[24] L. Amico, D. Aghamalyan, F. Auksztol, H. Crepaz, R. Dumke, and L. C. Kwek, Sci. Rep. **4**, 4298 (2014).
[25] D. Aghamalyan, M. Cominotti, M. Rizzi, D. Rossini, F. Hekking, A. Minguzzi, L.-C. Kwek, and L. Amico, New J. Phys. **17**, 045023 (2015).
[26] D. Aghamalyan, N. T. Nguyen, F. Auksztol, K. S. Gan, M. M. Valado, P. C. Condylis, L.-C. Kwek, R. Dumke, and L. Amico, New J. Phys. **18**, 075013 (2016).
[27] D. Aghamalyan, L. Amico, and L. C. Kwek, Phys. Rev. A **88**, 063627 (2013).
[28] A. C. Mathey and L. Mathey, New J. Phys. **18**, 055016 (2016).
[29] T. Haug, J. Tan, M. Theng, R. Dumke, L.-C. Kwek, and L. Amico, Phys. Rev. A **97**, 013633 (2018).
[30] A. Nunnenkamp, A. M. Rey, and K. Burnett, Phys. Rev. A **84**, 053604 (2011).
[31] M. Cominotti, D. Rossini, M. Rizzi, F. Hekking, and A. Minguzzi, Phys. Rev. Lett. **113**, 025301 (2014).
[32] A. Turpin, J. Polo, Y. V. Loiko, J. Küber, F. Schmaltz, T. K. Kalkandjiev, V. Ahufinger, G. Birkl, and J. Mompart, Opt. Express **23**, 1638 (2015).
[33] R. Dumke, Z. Lu, J. Close, N. Robins, A. Weis, M. Mukherjee, G. Birkl, C. Hufnagel, L. Amico, M. G. Boshier, K. Dieckmann, W. Li, and T. C. Killian, Journal of Optics **18**, 093001 (2016).
[34] V. E. Korepin, N. M. Bogoliubov, and A. G. Izergin, *Quantum Inverse Scattering Method and Correlation Functions*, Vol. 3 (Cambridge University Press, Cambridge, 1997).
[35] F. Haldane, Phys. Lett. A **80**, 281 (1980).
[36] T. Choy and F. Haldane, Phys. Lett. A **90**, 83 (1982).
[37] T. Choy, Phys. Lett. A **80**, 49 (1980).
[38] M. Valiente and D. Petrosyan, J. Phys. B: At. Mol. Opt. Phys. **41**, 161002 (2008).
[39] M. Valiente and D. Petrosyan, J. Phys. B: At. Mol. Opt. Phys. **42**, 121001 (2009).
[40] M. Valiente and D. Petrosyan, EPL (Europhysics Letters) **83**, 30007 (2008).
[41] M. Valiente, Phys. Rev. A **81**, 042102 (2010).
[42] Cristian Degli Esposti Boschi, E. Ercolessi, L. Ferrari, P. Naldesi, F. Ortolani, and L. Taddia, Phys. Rev. A **90**, 043606 (2014).
[43] J. Dalibard, *Quantum Matter at Ultralow Temperatures* (IOS Press, Amsterdam, 2015).
[44] R. Peierls, Z. Physik **80**, 763 (1933).
[45] A. J. Leggett, in *Granular Nanoelectronics*, edited by D. K. Ferry, J. R. Barker, and C. Jacoboni (Springer US, Boston, 1991), pp. 297–311.
[46] L. Amico and V. Korepin, Ann. Phys. **314**, 496 (2004).
[47] O. Dutta, M. Gajda, P. Hauke, M. Lewenstein, D.-S. Lühmann, B. A. Malomed, T. Sowiński, and J. Zakrzewski, Rep. Prog. Phys. **78**, 066001 (2015).
[48] X. Zotos and P. Prelovšek, *Strong interactions in Low Dimensions* (Springer Netherlands, Amsterdam, 2004), pp. 347–382.
[49] G. Arwas and D. Cohen, AIP Conf. Proc. **1912**, 020001 (2017).
[50] N. W. Ashcroft and N. D. Mermin, *Solid State Physics* (Cengage Learning, USA, 1976).
[51] S. Moulder, S. Beattie, R. P. Smith, N. Tammuz, and Z. Hadzibabic, Phys. Rev. A **86**, 013629 (2012).
[52] P. Naldesi, J. P. Gomez, B. Malomed, M. Olshanii, A. Minguzzi, and L. Amico, Phys. Rev. Lett. **122**, 053001 (2019).
[53] P. Naldesi, J. Polo Gomez, V. Dunjko, H. Perrin, M. Olshanii, L. Amico, and A. Minguzzi, arXiv:1901.9398.
[54] B. S. Shastry and B. Sutherland, Phys. Rev. Lett. **65**, 243 (1990).
[55] A. Osterloh, L. Amico, and U. Eckern, Nucl. Phys. B **588**, 531 (2000).